Available online at www.sciencedirect.com
SCIENCE DIRECT
Polymer 46 (2005) 751–760
polymer
www.elsevier.com/locate/polymer

Characterization on mixed-crystal structure of poly(butylene terephthalate/succinate/adipate) biodegradable copolymer fibers

X.Q. Shi, K. Aimi, H. Ito, S. Ando, T. Kikutani*

Department of Organic and Polymeric Materials, Graduate School of Science and Engineering, Tokyo Institute of Technology, 2-12-1, O-okayama, Meguro-ku, Tokyo 152-8552, Japan

Received 25 August 2004; received in revised form 18 November 2004; accepted 22 November 2004
Available online 8 December 2004

Abstract

Biodegradable poly(butylene terephthalate/succinate/adipate) (PBTSA) pellet, an ideal random copolymer characterized by ^{1}H solution NMR, was melt-spun into fibers. The crystal structure and physical properties of the as-spun fibers were investigated by WAXD, solid-state ^{13}C NMR, DSC and tensile test measurements. Only poly(butylene terephthalate) (PBT)-like diffraction pattern was observed in WAXD; however, two different ^{13}C spin-lattice relaxation time (T_{1C}) components were observed for aliphatic units, in which the longer and the shorter T_{1C} components correspond to the crystalline and the amorphous domains, respectively. Therefore the crystal structure of PBTSA was concluded to be formed by mixed crystallization of its comonomers. Such crystallization behavior enabled the PBTSA fibers to have well developed PBT-like crystal structure despite of its ideal randomness. Furthermore, due to the introduction of soft segments (BA and BS) into BT crystal lattice, melting temperature of PBTSA fibers (115 °C) was over 100 °C lower than that of PBT.

Keywords: Poly(butylene terephthalate/succinate/adipate) (PBTSA); Mixed crystallization; Molecular mobility

1. Introduction

With the growing awareness of environmental problems induced by plastics, many studies are being carried out on biodegradable polymers [1–8]. Biodegradable polymers can be classified into two major categories according to whether the starting materials are based on a petroleum source or a non-petroleum source. Compared with the non-petroleum polymers, petroleum based polymers are easily adaptable for mass production. Furthermore, polymers of various characteristics can be produced by utilizing recent advances in the field of polymer synthesis. Among petroleum based biodegradable polymers, great interest has been given to researches on aliphatic/aromatic copolymers that are designed to combine the biodegradability of aliphatic unit with the beneficial physical properties of aromatic unit [9–17]. For example, poly(butylene adipate-*co*-terephthalate) (PBAT, 'Ecoflex') is a commercial aliphatic/aromatic biodegradable polymer product from BASF. Its biodegradation behavior and properties have been reported by Müller et al. [11,13–14,17]. PBAT was characterized as an ideal random copolymer with a molar ratio of aliphatic to aromatic units around 1:1 [13]. It is obvious that polymer properties such as biodegradability, thermal property and mechanical property would also strongly depend on its crystal structure.

Recently, Doi et al. reported the crystallization behavior of PBAT [18]. From the results of solid-state ^{13}C NMR, the crystalline components of poly(butylene adipate) (PBA) homopolymer were found to have rigid methylene carbons; however, no such rigid methylene carbon was observed in PBAT copolymer. Hence, they concluded that only BT units were included in the crystalline region of PBAT, while BA units were excluded from the crystalline region.

More recently, Marchessault et al. also reported the crystalline structure of the same copolymer PBAT [19], and in contrast to the conclusion of Doi et al., they pointed out that both BT and BA units exist in crystalline region of PBAT copolymer. They found two kinds of BA components

* Corresponding author. Fax: +81 3 5734 2876.
E-mail address: tkikutan@o.cc.titech.ac.jp (T. Kikutani).

0032-3861/$ - see front matter © 2004 Elsevier Ltd. All rights reserved.
doi:10.1016/j.polymer.2004.11.080

with different molecular mobility in the solid-state ^{13}C NMR measurements. The more mobile BA component was assigned to be amorphous, while the less mobile one was assigned to be crystalline.

A study on a similar aliphatic/aromatic copolymer, poly(butylene adipate-*co*-succinate)/poly(butylene terephthalate) (PBAS/PBT), was reported by Park et al. [20]. They clarified that in PBAS/PBT block copolymer, only rich component can form crystal. When the molar ratio of aliphatic to aromatic units is about 1:1, neither aliphatic nor aromatic units can crystallize.

Summarizing the above, the reported studies on the crystallization behavior of aliphatic/aromatic copolymer (PBAT, PBAS/PBT) are not consistent. To investigate further the crystallization behavior of aliphatic/aromatic copolymers, the analysis of the crystalline structure of poly(butylene terephthalate/succinate/adipate) (PBTSA) was carried out in this research. Unlike the reported studies on aliphatic/aromatic copolymers, which were dealing with drawn and annealed film samples, in this work, PBTSA was melt-spun into fibers at a take-up velocity of 2000 m/min. There are few reports on aliphatic/aromatic biodegradable fibers till now, although these fibers have great demand in both the agricultural and medical fields. Therefore, this work is also expected to yield useful information on processing and properties of biodegradable PBTSA fibers.

2. Experimental

2.1. Materials and sample preparation

Terpolymer PBTSA was supplied in pellet by Ire Chemical Ltd, under the commercial brand name of Enpol-G8000 (MFI: 3–6 g/min, M_n: > 30,000, M_w: > 80,000). Its chemical structure is shown in Fig. 1.

PBTSA as-spun fiber was prepared through the melt-spinning process. The polymer was dried in vacuum at 60 °C for 12 h before the melt spinning to avoid possible hydrolysis during the extrusion process. The polymer was then extruded at 240 °C from a spinneret with four-holes of 0.5 mm diameter. The through-put rate was 1.24 g/min for each hole. The extruded fiber was then taken up at 2000 m/min by a high-speed winder placed about 300 cm below the spinneret. Poly(butylene terephthalate) (PBT) fiber prepared at the extrusion temperature of 240 °C and the take-up velocity of 8000 m/min was used as reference in this work.

2.2. ^{1}H solution NMR characterization

To investigate the composition and the sequence distribution of PBTSA, ^{1}H NMR measurements were carried out at room temperature using a JEOL GSX-500 spectrometer operated at a resonance frequency of 500 MHz. PBTSA pellets were dissolved in deuterated chloroform ($CDCl_3$), and tetramethylsilane (TMS) was used as an internal chemical shift standard in NMR spectrum.

2.3. Solid-state ^{13}C NMR measurements

Solid-state ^{13}C NMR CP/MAS, direct polarization (DP), and T1CP spectra were observed with JEOL EX spectrometer operated at 75.45 MHz. The rate of magic angle sample spinning (MAS) was set to 4.0–4.3 kHz for each measurement. The contact time for cross polarization (CP) was 2 ms, and the recycle delay was 5 s. CP/MAS was used to enhance the immobile signals compared with mobile ones. DP was used for selective observation of mobile phase with ^{13}C 45° pulse of 2.5 μs and recycle delay of 5 s. Torchia's T1CP pulse sequence was used to observe signals from immobile (crystalline) domain [21]. ^{13}C spin-lattice relaxation times, T_{1C}, for immobile and mobile phases were measured using T1CP and ^{13}C DP inversion recovery (IR) pulse sequences, respectively. The chemical shifts were calibrated indirectly through the adamantine peak observed at lower frequency (29.5 ppm) relative to TMS.

2.4. Differential scanning calorimetry (DSC)

The thermal property of PBTSA fiber was analyzed by using a differential scanning calorimeter (Shimadzu DSC-50). About 5 mg of PBTSA fiber sample which was cut into small pieces was encapsulated in aluminum DSC pans. The DSC measurement was carried out from room temperature to 250 °C at a heating rate of 10 K/min. The melting peak temperature (T_m) was obtained from the DSC thermogram. The DSC measurement of PBT fiber was also carried out for comparison.

2.5. Tensile test

A tensile testing machine (Toyosokki, UTM-4L) was used to obtain the stress–strain curve of single filament at room temperature. The gauge length was 20 mm and the tensile speed was 20 mm/min.

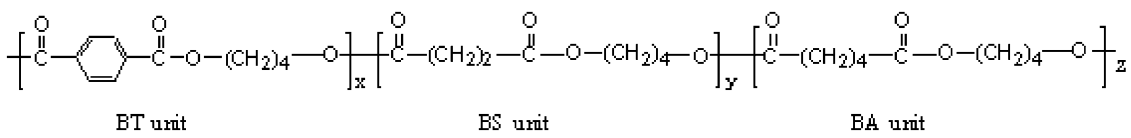

Fig. 1. Chemical structure of PBTSA terpolymer. BT, butylene terephthalate; BS, butylene succinate; and BA, butylene adipate.

2.6. Wide angle X-ray diffraction (WAXD) measurements

Wide angle X-ray diffraction (WAXD) patterns of the fiber bundle were obtained by using an X-ray generator (Rigaku Denki) and a CCD detector. The generator was operated at 40 kV and 300 mA, and a nickel-filtered Cu Kα radiation was used. The exposure time was set to 10 s×5 times. Measurements were carried out in three kinds of sample setting conditions: (a) in a relaxed state at room temperature, (b) under tensile stress at room temperature, and (c) in a relaxed state during a heating process.

For WAXD measurements under tensile stress, a mini tensile testing machine (Kyowa) was used to impose the tensile deformation. The tensile machine allowed symmetric deformation of the sample, which permitted the focused X-ray to illuminate the same sample position during stretching. About 1500 filaments were arranged parallel to each other at a width of 8 mm to obtain sufficient diffraction intensity. The gage length was 20 mm. The tensile speed was 20 mm/min. WAXD patterns were recorded at different tensile strains. Reflections close to the meridional direction were clearly monitored by tilting the fiber bundle properly in a plane containing the X-ray beam and the fiber bundle.

For WAXD measurements during a heating process, samples were set in a heating chamber. The temperature was increased from room temperature to 150 °C with a temperature controller. The heating rate was 1 K/min. The temperature was held for 2 min every 10 K, and the WAXD patterns were recorded during the holding period.

3. Results and discussion

3.1. Composition and sequence distribution analysis

Crystallization behavior in a copolymer system is inherently influenced by its chemical structure, such as comonomer composition and sequence distribution [22]. Hence, firstly composition and sequence distribution of the PBTSA pellet were investigated.

Fig. 2 shows the ^{1}H NMR spectrum of PBTSA. Peaks assignment was done by consulting a paper by Kang [20]. The chemical shifts of butylene protons were classified according to the sequences to its two ends. The definition of sequences AlAl, ArAr, ArAl and AlAr were given elsewhere [20]. By using the area ratio of the each characteristic peak, the molar fraction of aromatic BT, aliphatic BS and aliphatic BA units in the PBTSA were estimated to be 48, 26 and 26 mol%, respectively. It has been reported that the aliphatic/aromatic copolyester with a molar fraction of aromatic units at a range of 35–55 mol% offers an optimal compromise of its biodegradability and physical properties [14,17].

The sequence distribution of an aliphatic/aromatic copolymer is obtainable by analyzing the new proton signals due to the heterolinkage of aliphatic and aromatic units in its ^{1}H NMR spectrum [20,23]. A brief description of the process is given here. Each fraction of dyads (f_{AlAl}, f_{AlAr}, f_{ArAl}, and f_{ArAr}) can be calculated as the proportion of the integrated intensities of AlAl, AlAr, ArAl and ArAr signals.

$$f_{AlAl} = \frac{A_{AlAl}}{A_{AlAl} + A_{AlAr} + A_{ArAl} + A_{ArAr}} \quad (1)$$

$$f_{AlAr} = \frac{A_{AlAr}}{A_{AlAl} + A_{AlAr} + A_{ArAl} + A_{ArAr}} \quad (2)$$

$$f_{ArAl} = \frac{A_{ArAl}}{A_{AlAl} + A_{AlAr} + A_{ArAl} + A_{ArAr}} \quad (3)$$

$$f_{ArAr} = \frac{A_{ArAr}}{A_{AlAl} + A_{AlAr} + A_{ArAl} + A_{ArAr}} \quad (4)$$

The molar fraction of aliphatic units (P_{Al}) and aromatic units (P_{Ar}) would be

$$P_{Al} = \frac{(f_{AlAr} + f_{ArAl})}{2} + f_{AlAl} \quad (5)$$

$$P_{Ar} = \frac{(f_{AlAr} + f_{ArAl})}{2} + f_{ArAl} \quad (6)$$

The average block lengths of aliphatic unit ($\bar{L}_{nAl}$) and aromatic unit ($\bar{L}_{nAl}$) are given in Eqs. (7) and (8)

$$\bar{L}_{nAl} = \frac{2P_{Al}}{(f_{AlAr} + f_{ArAl})} \quad (7)$$

$$\bar{L}_{nAr} = \frac{2P_{Ar}}{(f_{AlAr} + f_{ArAl})} \quad (8)$$

The degree of randomness is defined by

$$B = \frac{1}{\bar{L}_{nAl}} + \frac{1}{\bar{L}_{nAr}} \quad (9)$$

In case of PBTSA, the chemical shifts of butylene protons are diagnostic of their chemical environments [20]. By using all the butylene protons related peaks, the sequence distribution of PBTSA was determined. $\bar{L}_{nAl}$ and $\bar{L}_{nAr}$ were analyzed to be 2.07 and 1.93, respectively. The degree of randomness of the PBTSA was 0.999, where unity is defined as the ideal randomness [24]. Therefore, the PBTSA used in this experiment can be regarded as an ideal random copolymer. It is notable that the average block length of BT units was 1.93. Since it has been reported that oligomers with less than 3 aromatic diesters can be attacked by microbes [13,25], the PBTSA is degradable not only in aliphatic units but also in most part of aromatic units.

3.2. Analysis on the structures of as-spun fibers

3.2.1. WAXD measurement at room temperature

Fig. 3 shows the WAXD patterns of (a) PBTSA as-spun fiber, (b) PBT as-spun fiber, and (c) the calculated PBT α-form crystal by using reported lattice unit parameters [26].

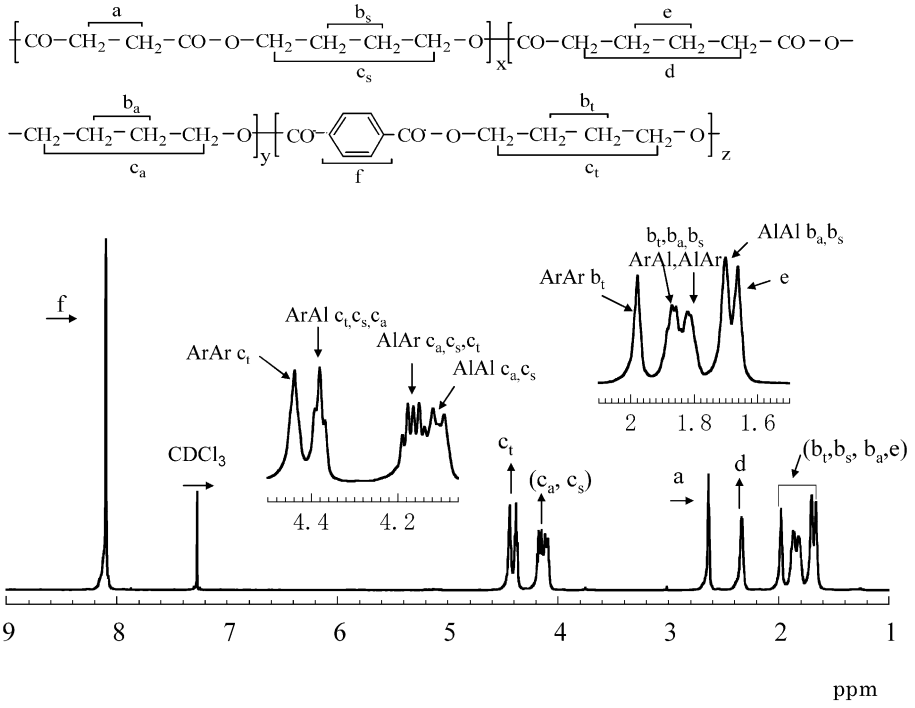

Fig. 2. 500 MHz ^{1}H NMR spectrum of PBTSA.

Although the PBTSA was analyzed to be an ideal random copolymer, distinct and fairly sharp reflection spots were observed in the WAXD pattern of PBTSA as-spun fiber, suggesting that it has well-developed and highly oriented crystal structure. Furthermore, it was found that the WAXD pattern of PBTSA fiber is similar to that of highly oriented α-form crystal of PBT. This fact led to the speculation that the crystal structure of PBTSA fiber was formed by its BT unit.

However, it was also reported that alternating copolymers poly(butylene terephthalate/succinate) (PBTS, or PTMTS) and poly(butylene terephthalate/adipate) (PBTA, or PTMTA) have similar crystal structure to that of PBT α-form crystal [27]. Table 1 shows the comparison of the observed and calculated lattice spacings (d_{obs} and d_{cal}). Spacing d_{obs} was analyzed using Bragg equation.

On the other hand, theoretical value for each *hkl* plane d_{cal} was calculated by using the lattice unit parameters of α-form PBT, PBTS and PBTA, respectively [26–27]. According to the result in Table 1, the possibility that aliphatic units (BA, BS) were included in BT crystal lattice in PBTSA fiber can not be excluded. Such crystallization behavior in a copolymer is defined as mixed crystallization, while co-crystallization is defined as the crystallization in which both co-monomers crystallize, but not necessarily form a common crystal lattice [28–30].

Based on the WAXD pattern of PBTSA fiber, quantitative analyses were also conducted on its crystallinity, crystalline orientation and crystallite size of (010), ($\bar{1}$10) and (100) planes (*hkl* was assigned according to the crystalline unit cell of α-form PBT). The crystallinity was estimated from the intensity fraction of total crystalline diffraction peaks to the total diffraction. Gaussian function was used to perform curve fitting for each crystalline

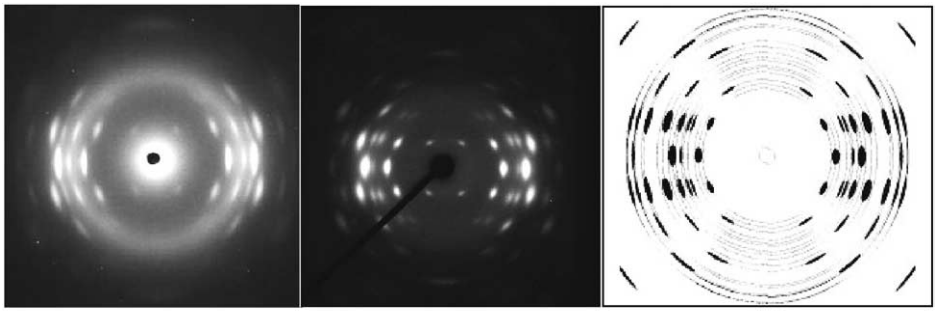

Fig. 3. WAXD patterns of PBTSA fiber, PBT fiber and calculated α-PBT according to its unit cell parameter [26].

Table 1
The comparison of the observed and calculated d spacing of PBTSA by using α-PBT, PTMTA and PTMTS unit cell parameters [27]

PBTSA	α-PBT		PTMTA		PTMTS	
d_{obs} (nm)	*hkl*	d_{cal} (nm)	*hkl*	d_{cal} (nm)	*hkl*	d_{cal} (nm)
0.511	010	0.513	010	0.507	010	0.507
0.418	$\bar{1}10$	0.418	$\bar{1}10$	0.417	$\bar{1}10$	0.418
0.376	$\bar{1}00$	0.383	100	0.380	100	0.377
0.541	$0\bar{1}1$	0.548	$0\bar{1}2$	0.555	$0\bar{1}2$	0.551
0.392	011	0.396	012	0.391	012	0.391
0.429	$\bar{1}11$	0.427	$\bar{1}12$	0.427	$\bar{1}12$	0.431
0.352	$1\bar{1}1$	0.352	$1\bar{1}2$	0.354	$1\bar{1}2$	0.350

diffraction peak. The integrated intensity was obtained from intensity distribution along diffraction angle 5–50° for various azimuthal angles (0–π/2). The degree of crystalline orientation is represented by practical orientation factor estimated using the half-width of the diffraction peak through azimuthal scan. The crystallite size, which is represented by the thickness of crystallite in the direction normal to each crystalline plane, was calculated using Scherer's equation [31]. The results listed in Table 2 confirmed that PBTSA fiber had well developed and highly orientated crystal structure. It is noteworthy that PBTSA fiber has the crystallite size up to 7.8 nm.

3.2.2. Mechanical properties

Fig. 4 shows the stress–strain curves of PBTSA and PBT fibers. It is notable that PBTSA exhibits a rubber-like stress–strain curve. The modulus and tensile strength of PBTSA fiber are remarkably lower compared with those of PBT fiber. The coexistence of aromatic rigid chain and aliphatic flexible chain in PBTSA along with relatively low crystallinity of about 25% may induce this elastomeric property, a phenomenon that has been widely reported in segmented polyurethane [32–33].

3.3. Detailed analyses of crystal structure characteristics

3.3.1. Thermal properties revealed by DSC

Fig. 5 shows the thermogram of PBTSA and PBT fibers in DSC measurement. Only one small and fairly broad endothermic peak was observed for PBTSA fiber during thermal scan from room temperature to 250 °C. The melting peak (T_m) was around 115 °C, which is about 100 °C lower than that of PBT fiber. Heat of melting analyzed for PBT and PBTSA fibers were 60 and 23 J/g, which corresponds to the crystallinity of 41 and 16%, respectively, if heat of melting for PBT perfect crystal of 145 J/g was assumed [34].

Table 2
Quantitative analysis results of crystalline structure of PBTSA fiber obtained from WAXD measurement

(*hkl*)	(010)	($\bar{1}10$)	(100)
Orientation factor	0.925	0.915	0.920
Crystallite size (nm)	6.0	3.5	7.8
Crystallinity	25%		

3.3.2. Crystal transition revealed by WAXD measurement

Based on the above described crystal structure analyses, and supposing that the crystalline structure of PBTSA fiber was formed by pure BT units, the crystal form transition was expected to occur during tensile deformation. The length of the repeating unit of fully extended PBT is about 1.35 nm, yet the unit cell length in c axis of α-form PBT is about 1.16 nm. The chain in the crystalline region of α-form is contracted, which leads to its interesting property of α to β (in fully extended state) crystal phase transition induced by tensile deformation [26,35–36]. On the other hand, the most characteristic crystallographic reflections in the PBT WAXD patterns are ($\bar{1}04$) at 31.4° and ($\bar{1}05$) at 39.5° for the α-form; and are ($\bar{1}04$) at 28.2° and ($\bar{1}06$) at 43° for the β-form, respectively. These characteristic reflections are generally used to judge the crystal phase of PBT. In order to check whether PBTSA fibers also undergo such crystal phase transition during tensile deformation, WAXD measurement under tensile stress was performed.

Fig. 6 shows the WAXD meridional profiles of PBTSA and PBT fibers measured in situ during tensile deformation. Firstly, PBTSA fibers showed the two characteristic diffraction peaks of PBT α-form at 31.4 and 39.5° (see Fig. 6(a) and (d)), which further confirms that PBTSA fiber has a similar crystal structure to that of PBT α-form.

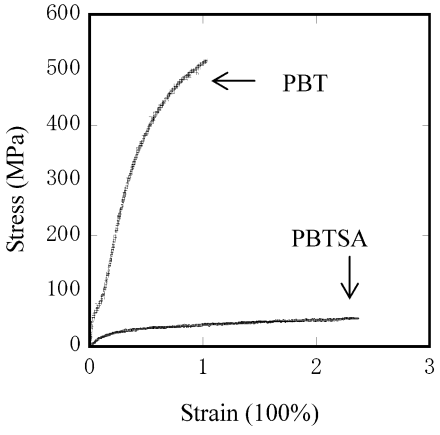

Fig. 4. Stress–strain curve of PBTSA and PBT fibers.

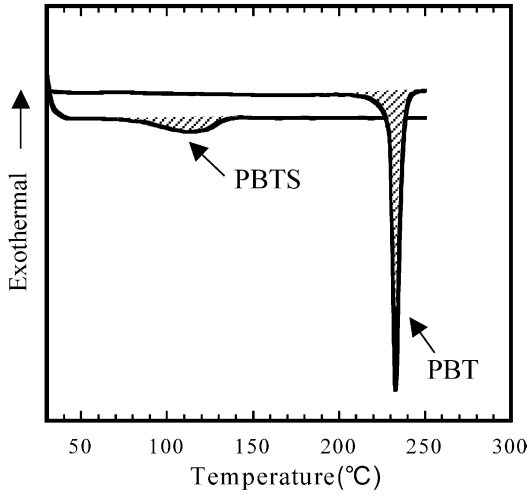

Fig. 5. DSC thermograms of PBTSA and PBT fibers.

Secondly, α to β crystal transition was clearly observed in PBT fibers with the increasing of strain (see Fig. 6(a)–(c)). Only β crystal form was observed when tensile strain arrived at 30%. However, no such change was observed in PBTSA fiber even when strain arrived at 45% (see Fig. 6(e)). WAXD pattern of PBTSA fiber at a further deformation was not obtained in this work due to the limitation of experimental set-up. It has been widely reported that α-form of PBT would totally change into β-form at a strain of 15% during tensile deformation [26,35–36]. However, there is one more important postulate for the occurrence of α to β transition besides the overall strain: only after the applied tensile stress arrives at a particular value f^* (critical stress), rather than the applied strain arrives at a particular value, will the α to β transition occur. According to Tashiro et al. [37], free energy of α-form becomes higher than that of β-form when the applied stress exceeds f^*, and the value of f^* depends on the temperature and is independent of crystallinity. At room temperature, f^* has been reported to be ca. 74.8 MPa [37]. In case of pure PBT polymer, when strain arrives at the region of 4–12%, the applied stress is generally higher than this critical stress. However, in case of PBTSA copolymer, because of its elastomeric property, applied stress was less than f^* even at tensile strain of 45% as revealed by its stress–strain curve in Fig. 4. In this context, non-existence of α to β crystal phase transition in PBTSA can not exclude the possibility of the existence of pure PBT crystal.

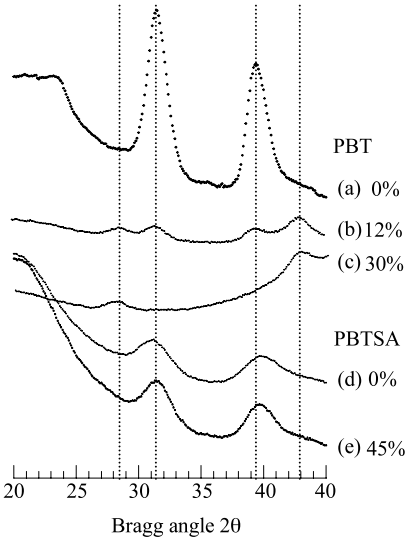

Fig. 6. WAXD meridional profiles of PBTSA and PBT fibers in situ during tensile deformation. Tensile strain as indicated.

3.3.3. Melting behavior

It is notable that PBTSA fiber has a well developed PBT-like crystal structure according to WAXD results; however, its T_m is significantly lower than that of PBT according to DSC results. In order to obtain more information on its melting behavior, WAXD patterns of PBTSA fiber was recorded in situ during its melting process.

In Fig. 7, the intensity of reflection spots started to decrease at ca. 105 °C, and completely disappeared at ca. 125 °C. Both DSC and WAXD measurements revealed that T_m of PBTSA fiber is around 115 °C, which is more than 100 °C lower than that of PBT. According to Flory [38–39], if only one kind of comonomer crystallizes in a random copolymer, the non-crystalline comonomer hinders the crystallization process. This leads to imperfect crystallite and hence leads to melting temperature depression. The melting temperature depression can be predicated as follows:

$$1/T_m^o - 1/T_m^* = -(R/\Delta H_m)\ln X \quad (10)$$

where T_m^o and T_m^* are the equilibrium melting temperatures of a random copolymer and the corresponding homopolymer of its crystallizable units, respectively. X is the molar fraction of crystallizable units, ΔH_m is the heat of fusion of the homopolymer of crystallizable units, and R is the gas constant. In case of PBTSA copolymer, T_m^* of PBT is 238 °C [40], ΔH_m is 145 J/g [34], X of BT units in PBTSA terpolymer revealed by ^{1}H NMR is 48 mol%.

T_m^o of PBTSA estimated from Eq. (10) is 180 °C, which is remarkably higher than the observed value of 115 °C. Distinct crystalline spots in WAXD pattern suggested that the PBTSA fiber has well developed crystal structure with fairly large crystallite size. If the crystal structure of PBTSA are formed by BT units only, such a striking melting depression seems unlikely to happen. In other words, another model of crystallization of PBTSA fiber is required to explain these experimental results.

In a random copolymer, there is a possibility of co-crystallization if the cohesive energies of each comonomer are identical [41]. In PBTSA, the cohesive energies of BT units (E_{aro}) and aliphatic units (BA and BS, E_{ali}) were estimated by group contribution methods [42]. The ratio of

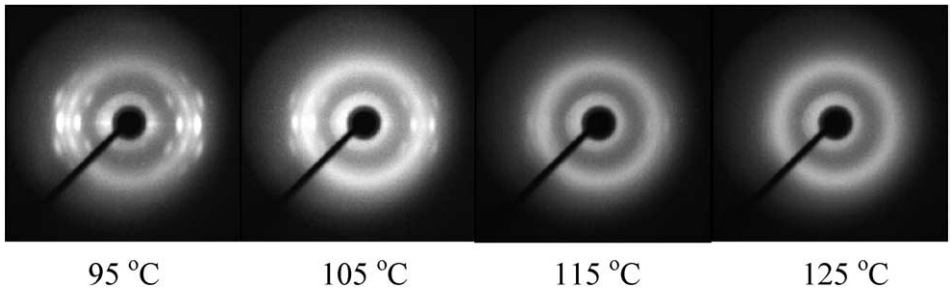

Fig. 7. WAXD patterns recorded in situ during a heating process at each temperature as indicated.

E_{aro} to E_{ali} was calculated to be 1.01, indicating that co-crystallization is possible in regard of dynamic stability.

As mentioned earlier, alternating copolymers PBTA and PBTS have been reported to be highly crystallizable and to have similar WAXD patterns to that of PBT [27]. It suggests that both BA and BS units can adjust their chain length to incorporate into BT crystal lattice. Thus, the spatial hindrance for mixed crystallization in PBTSA is negligible. Based on the above analyses, the crystalline structure of PBTSA should be formed more likely by mixed crystallization of BT units with other two aliphatic units.

3.4. Molecular mobility analyses by solid-state ^{13}C NMR measurement

Generally, WAXD is an effective way to characterize crystal structures; however, this analysis is based on geometrical regard rather than component regard. In contrast to WAXD, solid-state ^{13}C NMR can assign which component is included in the crystalline region by revealing molecular mobility. In general, two different ^{13}C spin-lattice relaxation time (T_{1C}) components are observed for semi-crystalline polymers above glass transition temperature, in which the longer and the shorter T_{1C} components correspond to the crystalline and the amorphous domains, respectively.

In case of PBTSA copolymer, WAXD measurements described above failed to assign crystallized component. Therefore, to find the direct evidence of mixed crystallization of BT units with BA and/or BS units in PBTSA fiber, solid-state ^{13}C NMR measurements were carried out.

3.4.1. Molecular mobility revealed by CP/MAS, DP and T1CP

Fig. 8 shows the ^{13}C CP/MAS, DP, and T1CP-4s NMR spectra for PBTSA fiber with peak assignments according to reported chemical shifts [18,43]. In the T1CP-4s spectrum (Fig. 8(c)), signals of the aromatic and carbonyl carbons were clearly observed, whereas those of the methylene carbons were not detected. This indicates that the methylene carbons have very short T_{1C}, and the methylene groups undergo vigorous molecular motion at the frequencies around several tens of MHz. In contrast, the aromatic and carbonyl carbons having longer T_{1C} do not undergo such high frequency motion. Further discussion for the molecular mobility and phase structures will be given below.

Fig. 9 shows the enlarged spectra of the carbonyl region of BT component in Fig. 8. The highest peak (165.9 ppm) in the amorphous-selective DP spectrum is resonated at higher frequency than that in the crystalline-selective CP/MAS and T1CP spectra (164.9 ppm). The chemical shift difference of 1.0 ppm indicates that there are two kinds of carbonyl carbons with different conformations. Hence, the BT units in PBTSA fiber should have both mobile (amorphous) and immobile (crystalline) components. However, the fact that a shoulder signal is also detected at 165.9 ppm in the CP/MAS and T1CP-4s spectra indicates that the difference in molecular motion between the crystalline and amorphous components is not so discrete.

Fig. 10 shows the ^{13}C T1CP spectra of PBA, PBS, and PBT homopolymers (PBS, PBA and PBT are commercial products from Aldrich company) together with that of copolymer PBTSA. Decay time (τ) in these measurements was 4 s. Firstly, all BT related peaks in PBTSA (Fig.10(d)) are observed in the same manner as those in PBT (Fig. 10(c)). Since the T_{1C} for the protonated aromatic carbons in the amorphous domain of PBT was reported to be ca. 0.53 s at room temperature [18], only crystalline signals should be observed for PBTSA. Thus, the signals observed at around 130 ppm confirmed that BT units in PBTSA have crystalline component. Secondly, all characteristic peaks of BS and BA units were clearly observed in the PBS and PBA spectra (Fig. 10(a) and (b)), indicating that all T_{1C} values of the crystalline components in PBS and PBA are longer than 4 s. This agrees with the reported data of PBA and PBS homopolymers [18,44]. In contrast, no signals relating to BS and BA units (peaks 'a'-'i' in Fig. 8) were observed for PBTSA fiber (Fig. 10(d)) except for a weak and broad signal resonated around 174 ppm given by the carbonyl carbons (peaks 'a' and 'e' in Fig. 8). It is notable that no methylene carbons were observed for PBT homopolymer (Fig. 10(c)) despite its high degree of crystallinity of ca. 40% determined by DSC. This observation agrees well with the report that there is no big difference between the T_{1C} values for methylene carbons in PBT whether they are in the crystalline region or in the amorphous region, both being less than 1 s [43]. This clearly indicates that the methylene carbons of PBT undergo vigorous molecular motion even in

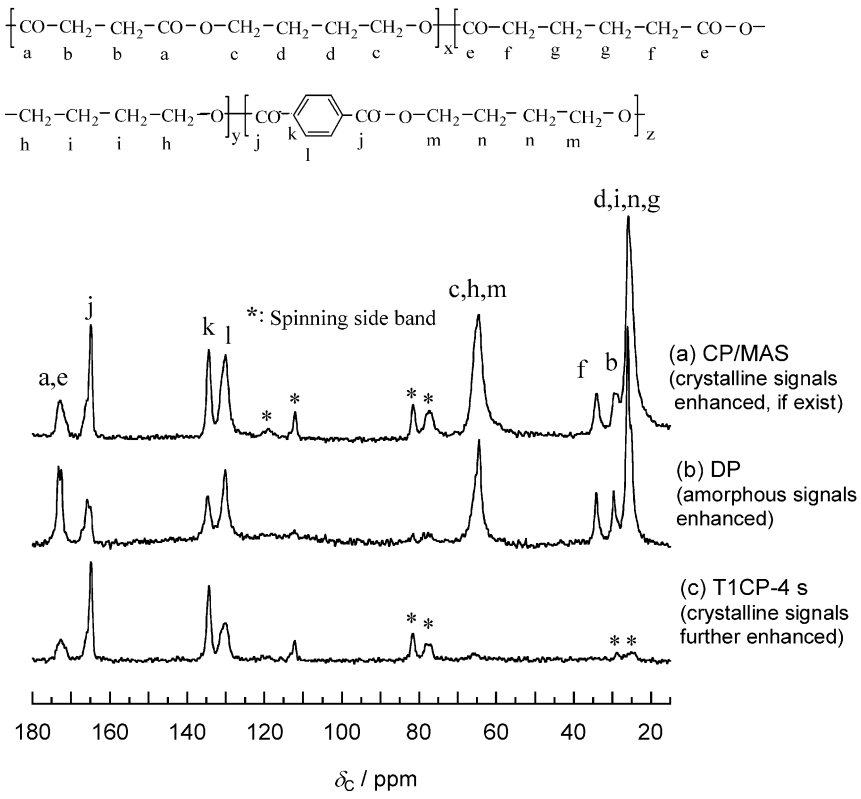

Fig. 8. Solid-state ^{13}C CP/MAS, DP and T1CP NMR spectra of PBTSA and signal assignments.

the crystalline region. The reason might be explained by considering the presence of the rigid and bulky benzene rings, which promotes the mobility of flexible methylene segments even in the crystalline region. Therefore, in case of aliphatic/aromatic copolymers, the molecular mobility of methylene carbons is not suitable to judge whether they are in the crystalline region or not. Considering the above, carbonyl carbons in PBTSA were examined to confirm whether BA and BS units have crystalline components.

3.4.2. Molecular mobility revealed by T_{1C} value

Fig. 11 shows the decays of the signals of aromatic and aliphatic carbonyl carbons observed by T1CP pulse sequence as a function of delay time τ. Integrals of Gaussian functions obtained by the deconvolution of observed signals to three peaks were used as signal intensities. The decays were fit using single exponential function. The obtained T_{1C} values are incorporated in Fig. 11.

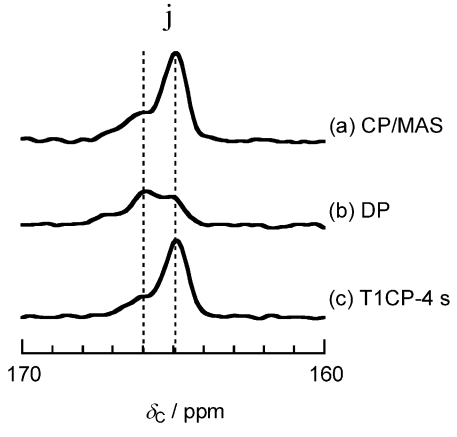

Fig. 9. Enlarged spectra of Fig. 8 in carbonyl carbon region of BT units.

The decay of the carbonyl peak for crystalline BT units resonated at 164.9 ppm (see Fig. 9) showed a long T_{1C} (39.6 s), whereas that for BA and BS units at 173.0 ppm exhibited relatively short T_{1C} (4.9 s). In addition, the T_{1C} of the shoulder peak for BT carbonyl signal resonated at 165.9 ppm (see Fig. 9(a) and (c)), which was assigned to the BT units in mobile domain, was slightly longer than that for the signals of BA and BS. These facts indicate that the carbonyl carbons of aliphatic BA and BS units are more mobile than that of the BT units both in the rigid crystalline and mobile amorphous domains. This view seems compatible with the phase structure proposed for PBAT copolymers by Doi et al., in which the BA units were excluded from the crystalline domain, and therefore the crystalline domain consisted of only BT units [18]. However, as shown in Fig. 8, the spectral shape of carbonyl signal of BA and BS units in DP spectrum (peaks ‘a’ and ‘e’) were obviously different from that in CP/MAS. Two sharp peaks with the same intensities were observed only in the DP spectrum but not in the CP/MAS spectrum. This strongly suggests that BA and BS units in PBTSA have some less mobile

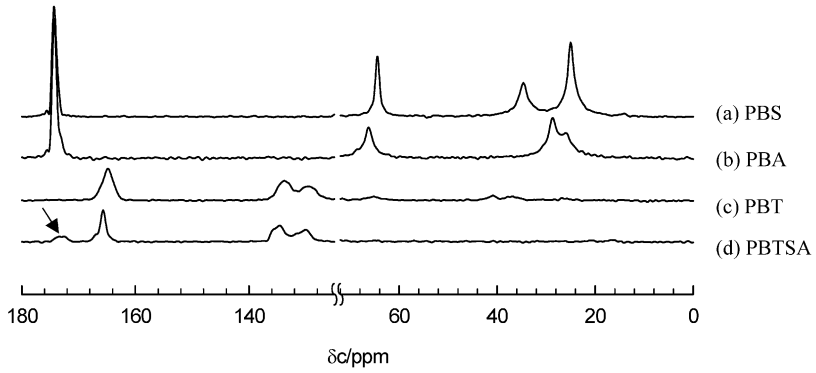

Fig. 10. T1CP spectra of PBA, PBS, PBT and PBTSA, decay time $\tau = 4$ s.

components compared with the components observed in DP spectrum. Therefore BA and BS units must have two kinds of T_{1C} values.

In order to estimate the T_{1C} of the mobile components that could not be detected by CP pulse sequence, ^{13}C DP measurements followed by inversion recovery (IR) were conducted. Fig. 12 shows the T_{1C} decays of the carbonyl peaks for BA, BS, and BT units obtained by IR pulse sequence as a function of delay time τ. The estimated T_{1C} values were incorporated in Fig. 12. The T_{1C} of carbonyl peaks at 173.4 and 172.6 ppm were shorter than those observed by T1CP pulse sequence (Fig. 11), which clearly indicates that two different domains exist for the BA and BS units in PBTSA. One is located in the mobile amorphous domain that can be detected only by IR pulse sequence. The other is located in the less-mobile (crystalline) region that can be detected only by CP and T1CP pulse sequence. On the other hand, the T_{1C} decay of the carbonyl peak for BT units (165.9 ppm) also contains a shorter component (5.4 s) than that detected by T1CP measurement (9.0 s). In contrast, the carbonyl signal for BT units in the crystalline domain (164.9 ppm) exhibits a much longer T_{1C} value (39.6 s). These findings indicate that there are three different components for BT units in PBTSA, the component with middle value of T_{1C} (9.0 s) was assigned to be in the interfacial region between the crystalline and the amorphous domain.

4. Conclusions

PBTSA pellet was characterized to be an ideal random copolymer. The molar ratio of its aliphatic units to aromatic units was found to be around 1:1. Such kind of copolymer is generally non-crystallizable. However, PBTSA fiber showed well-developed PBT-like crystal structure as revealed by WAXD, yet its T_m (115 °C) was over 100 °C lower than that of PBT. This unusual phenomenon was

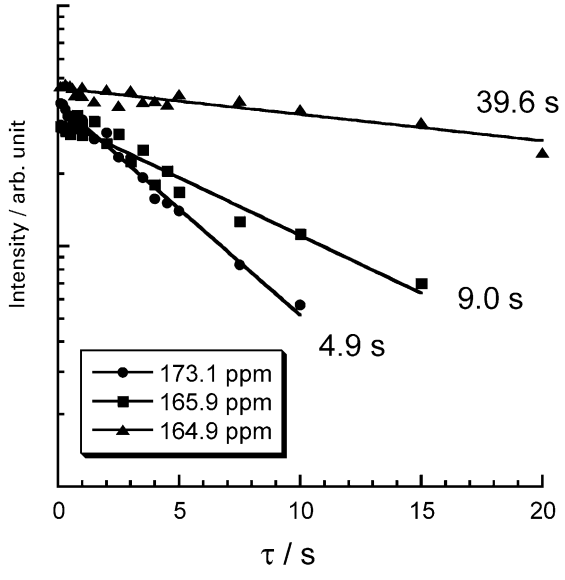

Fig. 11. The decays of the carbonyl signals observed by T1CP pulse sequence as a function of delay time τ. Peaks at 164.9, 165.9 and 173.1 ppm can be assigned to rigid, less rigid carbonyl carbon of BT unit, and rigid carbonyl carbons of BA/BS units, respectively.

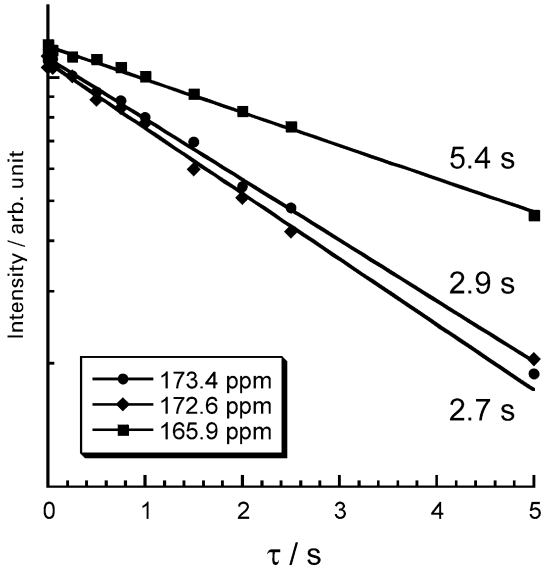

Fig. 12. The decays of the carbonyl signals obtained by IR pulse sequence as a function of delay time τ. Peaks at 165.9, 172.6/173.4 ppm can be assigned to mobile carbonyl carbons of BT unit and BA/BS units.

speculated to be caused by the mixed crystallization of comonomers in PBTSA fiber.

Mixed crystallization in PBTSA fiber was concluded based on the results of WAXD, DSC and solid-state ^{13}C NMR. Only PBT-like diffraction spots could be observed in WAXD patterns of PBTSA fiber, indicating that its crystal lattice dimension is similar to that of PBT α-form crystal. However, molecular mobility analyzed by ^{13}C NMR measurement revealed that both aromatic unit (BT) and aliphatic units (BA, BS) have crystalline components. These crystalline components detected by CP pulse sequence have longer T_{1C} values (4.9 s for BA/BS and 39.6 s for BT units) compared with the non-crystalline components detected by DP pulse sequence. Therefore, a part of aliphatic units (BA, BS) must be in a common crystal lattice with BT unit, where BA and BS units are incorporated into the crystal lattice of BT units.

References

[1] Doi Y. In: Microbial polyesters. New York: VCH Publishers; 1990.
[2] Lenz RW. Adv Polym Sci 1993;107:1.
[3] Doi Y, Fukuda K, editors. Biodegradable plastics and polymers. Amsterdam: Elsevier; 1994.
[4] Amass W, Amass A, Tighe B. Polym Int 1998;47:89.
[5] Sudesh H, Abe H, Doi Y. Prog Polym Sci 2000;25:1503.
[6] Chiellini E, Solaro R, editors. Macromol Symp, 2003. p. 197.
[7] Scott G. Polym Degrad Stab 2000;68:1.
[8] Okada M. Prog Polym Sci 2002;27:87.
[9] Maeda Y, Maeda T, Yamaguchi K, Kubota S, Nakayama A, Kawasaki N, Yamamoto N, Aiba S. J Polym Sci: Part A: Polym Chem 2000;38:4478.
[10] Jin H-J, Lee B-Y, Kim M-N, Yoon J-S. Eur Polym J 2000;36:2693.
[11] Rantze E, Kleeberg I, Witt U, Müller R-J, Deckwer W-D. Maromol Symp 1998;130:319.
[12] Yoo ES, Im SS. Macromol Symp 1997;118:739.
[13] Witt U, Müller R-J, Deckwer W-D. Maromol Chem Phys 1996;197:1525.
[14] Witt U, Müller R-J, Deckwer W-D. J Environ Polym Degrad 1995;3(4):215.
[15] Ki HC, Park OOk. Polymer 2001;42:1849.
[16] Müller R-J, Kleeberg I, Deckwer W-D. J Biotech 2001;86:87.
[17] Witt U, Müller R-J, Deckwer W-D. J Environ Polym Degrad 1997;5(2):81.
[18] Kuwabara K, Gan Z, Nakamura T, Abe H, Doi Y. Biomacromolecules 2002;3:390.
[19] Cranston E, Kawada J, Raymond S, Morin FG, Marchessault RH. Biomacromolecules 2003;4:995.
[20] Kang HJ, Park SS. J Appl Polym Sci 1999;72:593.
[21] Torchia DA. J Magn Reson 1978;30:613.
[22] Baur VH. Makromol Chem 1966;98:297.
[23] Yamadera R, Murano M. J Polym Sci 1967;5:2259.
[24] Bovey FA, Tiers GVD. J Polym Sci 1960;44:173.
[25] Witt U, Müller R-J, Deckwer W-D. J Environ Polym Degrad 1996;4(1):9.
[26] Yokouchi M, Sakakibara Y, Chatani Y, Tadokoro H, Tanaka T, Yoda K. Macromolecules 1976;9(2):266.
[27] Atfani M, Brisse F. Macromolecules 1999;32:7741.
[28] Bluhm TL, Hamer GK, Marchessault RH, Fyfe CA, Veregin RP. Macromolecules 1986;19:2871.
[29] Helfand E, Lauritzen Jr JI. Macromolecules 1973;6(4):631.
[30] Wunderich B. Macromol Phys. vol. 1. New York: Academic Press; 1973 [chapter 2–4].
[31] Scherrer P. Goettinger Nachrichten 1918;2:98.
[32] Wang CB, Cooper SL. Macromolecules 1983;16:775.
[33] Kimura I, Ishihara H, Ono H, Yoshihara N, Nomura S, Kawai H. Macromolecules 1974;7(3):355.
[34] Wunderlich B. In: Macromol Phys, vols. 2 and 3. New York: Academic Press; 1976. p. 1980.
[35] Al-jishi R, Taylor PL. Macromolecules 1988;21:2240.
[36] Jakeways R, Smith T, Ward IM, Wilding MA. J Polym Sci, Polym Lett 1976;14:41.
[37] Tashiro K, Nakai Y, Kobayashi M, Tadokoro H. Macromolecules 1980;13:137.
[38] Flory PJ. Trans Faraday Soc 1955;51:848.
[39] Marrs W, Peters RH, Still RH. J Appl Polym Sci 1979;23:1077.
[40] Chishholm BJ, Zimmer JG. GE Research Development Center, 2000CRD002; 2000.
[41] Yoo HY, Umemoto S, Kikutani T, Okui N. Polymer 1994;35:117.
[42] van Krevelen DW. Properties of polymers. Amsterdam: Elsevier; 1990 [chapter 7].
[43] Gomez MA, Cozine MH, Tonelli AE. Macromoleules 1988;21:388.
[44] Kuwabara K, Gan Z, Nakamura T, Abe H, Doi Y. Biomacromolecules 2002;3:1095.